

## MATERIALS SCIENCE

Special Topic: Energy Storage Materials

**Progress of rechargeable lithium metal batteries based on conversion reactions**Sen Xin<sup>1,†</sup>, Zhiwen Chang<sup>2,†</sup>, Xinbo Zhang<sup>2,\*</sup> and Yu-Guo Guo<sup>1,3,\*</sup>**ABSTRACT**

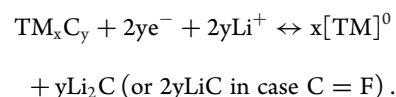
In this review, we focus on the conversion reaction in newly raised rechargeable lithium batteries instanced by lithium–sulfur and lithium–oxygen batteries. A comprehensive discussion is made on the fundamental electrochemistry and recent advancements in key components of both types of the batteries. The critical problems in the Li–S and Li–O<sub>2</sub> conversion electrochemistry are addressed along with the corresponding improvement strategies, for the purpose of shedding light on the rational design of batteries to reach optimal performance.

**Keywords:** energy storage, conversion reaction, lithium–sulfur battery, lithium–oxygen battery

**INTRODUCTION**

More than two decades have passed since the successful marketing of lithium–ion batteries for consumer electronics. Despite a steadily improved performance, the industry is now struggling to meet the increasing demand for energy and power outputs, so that the batteries can be applied to emerging fields including grids and automobiles. In a typical Li–ion battery, both electrodes (e.g. LiCoO<sub>2</sub> and LiFePO<sub>4</sub> for cathode and graphite for anode) are operated based on a Li intercalation reaction, during which Li ions are reversibly inserted into and extracted from the lattice of the electrode material, so that they can migrate back and forth in the battery to enable a charge–discharge cycle [1]. However, with theoretical limitations on capacities of intercalation-type electrode materials, it becomes extremely hard to further increase the energy density of batteries. In the search for materials with new functional mechanisms to make a breakthrough, those that can make ‘conversion’ reactions with lithium, such as binary transitional metal oxides and sulfides, have attracted great attention. As proposed by Armand *et al.*, the conversion electrochemistry versus Li of the materials with a general formula (TM<sub>x</sub>C<sub>y</sub>, where ‘TM’ denotes the transitional metal cations and ‘C’ denotes counteranions such as O<sup>2-</sup>, S<sup>2-</sup>, F<sup>-</sup>, etc.) is described

by the following equation [1–9]:



Through a multi-electron transfer process, the conversion-type materials can easily host more Li ions to reach specific capacities two to several times higher than those of intercalation-type materials, making them appealing choices to build high-energy rechargeable Li batteries. With an extensive study on the mechanism of electrochemical reactions, the concept of conversion has been extended from electrode materials to some newly emerging rechargeable Li battery systems, such as lithium–sulfur batteries and lithium–oxygen batteries [10–12]. In these batteries, the conversion reactions mainly occur on the cathode side, and these reactions do not strictly follow the conversion route for metal sulfide/oxide anodes. In the Li–S battery, S is directly reduced by Li to generate the sole product, lithium sulfide (Li<sub>2</sub>S), while, in the Li–O<sub>2</sub> battery, O<sub>2</sub> is reacted with Li to generate LiOH (with aqueous electrolyte) or Li<sub>2</sub>O<sub>2</sub> (with non-aqueous electrolyte) [11]. In both cases, there is no formation of metal particles by the end of discharge. However, in view of

<sup>1</sup>CAS Key Laboratory of Molecular Nanostructure and Nanotechnology, Institute of Chemistry, Chinese Academy of Sciences (CAS), Beijing 100190, China;

<sup>2</sup>State Key Laboratory of Rare Earth Resource Utilization, Changchun Institute of Applied Chemistry, Chinese Academy of Sciences, Changchun, 130022, China and <sup>3</sup>School of Chemistry and Chemical Engineering, University of Chinese Academy of Sciences, Beijing 100049, China

<sup>†</sup>Equally contributed to this work.

\*Corresponding authors. E-mails: [xbzhang@ciac.ac.cn](mailto:xbzhang@ciac.ac.cn); [yguo@iccas.ac.cn](mailto:yguo@iccas.ac.cn)

Received 12 September 2016;

Revised 25 October 2016; Accepted 2 November 2016

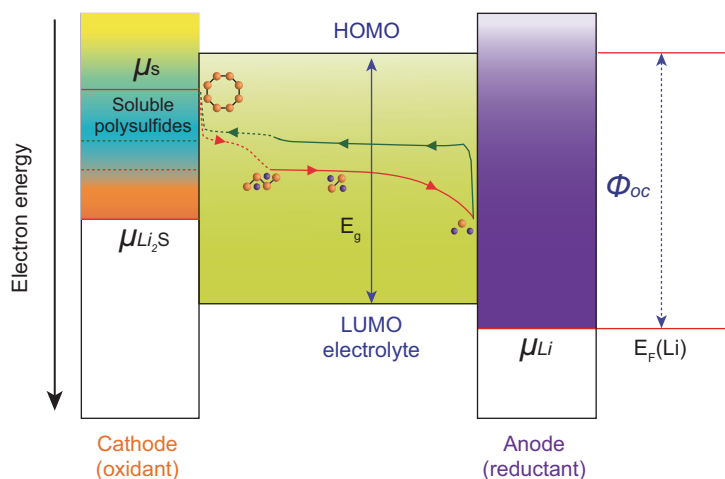


**Figure 1.** Electrochemistry of a Li–S battery based on cyclo- $S_8$ .  $\mu_S$ ,  $\mu_{Li_2S}$  and  $\mu_{Li}$  denote the chemical potential of S,  $Li_2S$  and Li, respectively, and LUMO and HOMO are short for the lowest unoccupied and highest occupied molecular orbitals of the electrolyte. Reproduced with permission from [12] (copyright 2013, Wiley-VCH).

the equivalent capacity-contributing component of ‘S’ and ‘O’, and the similar multi-electron redox process with breaking/reformation of the Li–S or Li–O bond, the electrochemistry of S/ $O_2$  versus Li are essentially the same as the reactions between metal sulfide/oxide with Li. With such conversion reactions, both electrodes are endowed with theoretical capacities at least one order of magnitude higher than those of the intercalation-type electrodes, so that the batteries hold promising energy outputs to power the oncoming ‘post-lithium’ era. In the following parts, we will go deep into the conversion reactions of Li–S and Li– $O_2$  batteries, revealing the fundamental science and key problems in their electrochemistry. Meanwhile, we will review the strategies for stabilizing the Li–S ( $O_2$ ) electrochemistry and the recent proceedings in the core components (e.g. electrodes and electrolytes) of both battery systems.

## LITHIUM–SULFUR BATTERY

### Introduction to the lithium–sulfur battery

Emerging in the 1960 s, the Li–S battery was considered theoretically promising yet practically underestimated in its competition with the Li–ion battery [10–12]. The turning point was in the year 2009, when Nazar’s group first demonstrated a cyclable prototype Li–S battery with impressive capacity output to trigger resurgent research interests thereafter [13]. Being complimented as a fascinating solution to next-generation energy storage, the cost and energy advantages of the Li–S battery, compared with the well-established Li–ion battery technology, are prominent [11,12,14–16]. With a rich

abundance and low price, the use of S as the cathode is expected to offset the resource and cost inferiority of Li and contributes to better sustainability [11,12,14–17]. Meanwhile, the high theoretical specific capacities of Li (3860 mA h/g) and S (1672 mA h/g) offset the relatively low voltage output of battery (2.1 V on average) and render a theoretical specific energy ( $\sim 2600$  W h/kg) five times higher than that of a graphite||LiCo $O_2$  battery ( $\sim 390$  W h/kg) [11,12]. Promising as this is, the reality is still far from satisfactory [18]. The Li–S conversion reaction that brings the high capacities also brings unstable electrochemistry with deteriorated performance of both electrodes. To stabilize the conversion reaction, considerable efforts have been made on improving the cathode/anode electrochemistry with proper structure design of electrode materials, updated electrolyte ingredients, and use of novel separators and current collectors. The following sections will discuss from an electrochemical view the recent advances in the key components of Li–S batteries.

### Strategies to improve sulfur electrochemistry

#### Electrochemistry of cyclooctasulfur

Due to the flexibility and variability of S–S bonds, S can form a large number of allotropes by catenation, among which homoatomic chains and cyclic rings are the two most common configurations. Cyclooctasulfur (cyclo- $S_8$ ), with an octatomic ring-like configuration, is the most stable allotrope, crystallizing as orthorhombic  $\alpha$ - $S_8$  at room temperature [19]. The electrochemistry of cyclo- $S_8$  with Li is actually a stepped reduction of S by Li, as Li holds a higher chemical potential than S (Fig. 1) [12,14–16]. The Li–S reaction in the compatible ether electrolytes starts with a ring-opening reaction, forming high-order lithium polysulfides  $Li_2S_x$  ( $6 < x \leq 8$ ). With a further uptake of Li, a chain-shortening reaction occurs to generate low-order lithium polysulfides  $Li_2S_y$  ( $2 \leq y \leq 6$ ) and finally  $Li_2S$  (Fig. 1) [12,14,15]. The Li release from  $Li_2S$  is completely reversible:  $Li_2S$  is first oxidized to various low-order polysulfides, then to high-order polysulfides and finally back to cyclo- $S_8$  [12,14,15]. The complicated multiphase conversion between various intermediates in the Li–S reaction generates two plateaus in the discharge/charge profiles of the battery (Fig. 1) [12,14]. The plateau with a higher voltage (usually starts at 2.35 V and ends at 2.0 V) corresponds to the conversion between  $S_8$  and  $Li_2S_4$ , and the other plateau with a lower voltage (usually starts at 2.0 V) corresponds to the conversion between  $Li_2S_4$  and  $Li_2S$  (Fig. 1) [12,14]. The polysulfides (especially the high-order

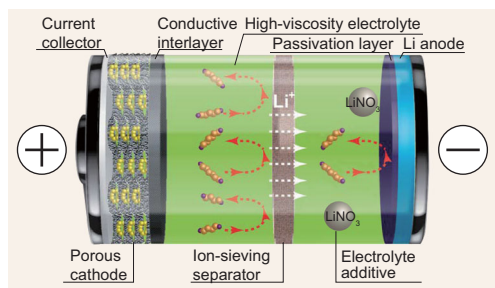


**Figure 2.** Summary of strategies to improve the electrochemistry of cyclo-S<sub>8</sub> cathode.

ones) generated during the above conversion process are easily soluble in ether electrolytes, which results in an irreversible active material loss from the cathode and, further, a significant shuttle of S species onto the anode surface, reduced and forming a passivation layer to inactivate the anode [12,14–16]. Hence, a continuous fade in capacity is almost unavoidable during repeated discharge/charge cycles. In this way, an effective trapping of soluble polysulfides on the cathode side has become one of the key issues in stabilizing the S electrochemistry.

### Strategies to improve S<sub>8</sub> electrochemistry

S confinement in a porous substrate has been reported as the most popular strategy to stabilize the S electrochemistry (Fig. 2) [12,14–16]. In the pioneering work by Ji *et al.*, S is confined in an ordered mesoporous carbon named CMK-3, which captures and maintains the soluble polysulfides via capillary actions during cycling so that the lifespan of the battery is extended [13]. Since then, substrates of different chemical compositions and nanostructures have been designed and synthesized to optimize the performance of the S cathode. Generally, these substrates have several features in common. First, these substrates should have sufficient electronic conductivity to compensate for the low conductivity of S. Carbon materials, such as pyrolysis carbon, carbon nanotubes and graphene, are ideal components to construct such porous substrates due to their high electronic conductivity and favorable electrolyte wettability, which enable fast e<sup>-</sup>/Li<sup>+</sup> transmissions for the electrochemical lithiation/delithiation of S [12,17,20–27]. In recent work by Zhang *et al.*, they used a graphene sheet loaded with highly graphitized sp<sup>2</sup> carbon nanocages as an efficient S host [23]. Each nanocage is surrounded by few-layered graphene shells and serves as a highly efficient electrochemical reactor for S and also a polysulfide reservoir [23]. With a full coverage of graphitic nanocages on the graphene backbone, a highly conductive and robust sp<sup>2</sup> carbon framework is formed, which ensures rapid electron trans-

port and structure stability of the S–C composite, and leads to superior cycling/rate performance of cathode at a high S loading [23]. The combination of carbon with nitrogen (from N doping to recent use of C<sub>3</sub>N<sub>4</sub>) or boron has been reported to significantly raise the conductivity of carbon substrates, which may be beneficial to improve the electroactivity and rate performance of S [22,28–30]. Transitional metal oxides of a semiconductor nature, such as TiO<sub>2</sub> or MnO<sub>2</sub>, have also been reported for S hosting since their electronic conductivities still meet the practical demands of a battery [31,32]. Second, these substrates should have appropriate porous structure, and strong chemical interactions (e.g. S interactions with Au or metal oxide) with the polysulfides so that active S species can be maintained on the cathode side via chemisorption [13,20–25,27,29,31,33,34]. Given that the S species may escape from the openings on the substrate surface, a conductive polymer layer is preferably coated outside to further enhance the restriction of S [13,35]. Third, the porous structure should be provided with enough void space to achieve a high S loading and sufficient flexibility to accommodate the 80% volume variation of S during Li intercalation [12,15]. Carbon substrates with hollow structures, such as spherical hollow carbons, are preferential choices, since they can maximize the sulfur mass loading and effectively alleviate the surface tension during the Li uptake of S [31,36,37]. This point has been verified by Zhou *et al.* in their *in situ* transmission electron microscopic observations on the lithiation of S inside mesoporous hollow carbon spheres [36].

To stabilize the electrochemistry of cyclo-S<sub>8</sub>, attention has also been given to the electrolytes, separators and current collectors (Fig. 2) [12,15]. Carbonate electrolytes have been reported as incompatible with cyclo-S<sub>8</sub> due to an unfavorable nucleophilic reaction between high-order polysulfides and carbonate solvent molecules [38]. However, recent work by Markevich *et al.* shows that the fluoroethylene carbonate electrolyte can trigger a better cycling performance of Li–S batteries by forming a solid electrolyte interface on the cathode surface to prevent polysulfide dissolution [39]. On the other hand, ether electrolytes have been reported as compatible with the cyclo-S<sub>8</sub> cathode yet suffering from significant dissolution and shuttle of polysulfides [12,15]. To ensure complete wetting of electrodes and avoid active S dissolution, the use amount of electrolyte is an important trick. Meanwhile, additives such as lithium nitrate (LiNO<sub>3</sub>) with anode passivation ability are added, with favorable results observed on shuttle suppression [40]. Other types of electrolytes, such as ‘solvent-in-salt’ electrolytes,

ionic liquid electrolytes and solid-state electrolytes, are also employed [41–44], and excellent shuttle prevention effects are observed, yet conductivity and cost concerns have still been raised before their practical use.

Commercial polymeric separators are effective in benefiting  $\text{Li}^+$  access while preventing an internal short circuit of battery, yet are invalid for preventing polysulfide migrations due to their oversized pore structures [15]. However, if narrowing down the pore size of the separator into tens or several nanometers, they may help in trapping the polysulfides during their shuttle. Recently, Bai *et al.* have reported a metal-organic framework (MOF)-based battery separator, which acts as an ionic sieve to selectively enable passing through of  $\text{Li}^+$  ions while efficiently suppressing undesired polysulfides migrating to the anode side. With the use of such a separator, a cathode with 70 wt% S exhibits a low capacity decay of 0.019% per cycle over 1500 cycles without any apparent capacity fade after the initial 100 cycles [45]. In the series of work by Manthiram's group, they have proposed a new cell configuration by adding a polysulfide-interception conductive interlayer between the cathode and the separator [15,46–48]. Such an interlayer, according to their claims, can effectively trap the dissolved polysulfides while improving the electric contact of S on the top of cathode, enabling a reduced carbon fraction in the cathode [46–48]. However, this layer of separator should be light and thin enough so that it will not deteriorate the practical gravimetric/volumetric energy output of the battery.

Aluminum foil is widely used as the current collector for the cathode in Li-ion batteries, yet suffers from corrosion by ether electrolytes and may account for the self-discharge of Li-S batteries [49,50]. Meanwhile, the Al collector should be used along with many other components, such as the binder and the carbon black as conductive additives to prepare the cathode, but these components usually have zero capacity contribution to the battery. As this inevitably lowers the active S content of the cathode (e.g. a cathode consisting of 80 wt% S-C composites ( $w_S:w_C = 7:3$ ), 10 wt% binder and 10 wt% carbon black coated on a 25- $\mu\text{m}$ -thick Al foil only has 34 wt% sulfur in the cathode), the composite capacity of the cathode and the specific energy of the battery is deteriorated. Targeting the above problems, S cathodes with integrated current collectors turn out to be wise choices. In the recent work by Jin *et al.*, they have designed a 3D current collector consisting of covalently-connected  $\text{sp}^2$  carbon bundles with gaps of 2–3 nm [51]. Sulfur is directly introduced into the nanogaps of the current collector to form an integral cathode without additions of binder and carbon black, so that a total S content of

43 wt% is achieved on the cathode with an areal loading density of 2.4  $\text{mg}_S/\text{cm}^2$  [51]. Benefiting from the highly conductive  $\text{sp}^2$  carbon network, the S cathode is able to deliver a reversible capacity of 860 mA h/g at 12 C rate, which corresponds to a specific power of 8680 W/kg with a specific energy of 720 W h/kg, showing an admirable prospect if a cost reduction and scalable synthesis of such a carbon collector can be realized [51].

### Novel sulfur electrochemistry

Though substantial efforts have been devoted to improving the electrochemistry of cyclo- $\text{S}_8$ , its inherent electrochemical instability versus Li is never changed. With abundant allotrope forms of S, it is natural to consider the possibility of other S candidates. In early work by Zhang *et al.*, S is loaded in microporous carbon spheres to strengthen the S-C interaction for an extended cycle life [52]. A different discharge-charge profile of S with suppressed voltage at a lower plateau is observed, which the authors ascribe to highly dispersed low-molecular S allotropes inside the C micropores [52]. However, it is not until the year 2012 that Guo's group first discovers the electrochemistry of chain-like  $\text{S}_{2-4}$  molecules metastably confined in slit pores of a microporous carbon with an average pore diameter of  $\sim 0.5$  nm (Fig. 3a) [21]. The small  $\text{S}_{2-4}$  molecules confined in microporous carbon are completely different allotropes from the conventional cyclo- $\text{S}_8$  with a dominating natural abundance. Due to their metastable nature, they exhibit an ultrahigh electrochemical activity versus Li, so that an almost complete Li-S reaction occurs to yield a specific capacity of S cathode close to its theoretical value during the initial discharge [21]. With a different initial electrochemical state, the  $\text{S}_{2-4}$  molecules effectively eliminate the conversion between cyclo- $\text{S}_8$  and  $\text{S}_4^{2-}$  during Li uptake/release by outputting a single plateau at about 1.9 V in its voltage profile (Fig. 3a) and is completely compatible with the carbonate electrolyte [21]. In this way, the generation of high-order polysulfides is avoided, which essentially solves the key problem of polysulfide dissolution and shuttle [21]. As a result, the cathode based on these small S allotropes exhibits an ultrahigh specific capacity, and excellent cycling/rate performance [21]. Li *et al.* further confirm that the lithiation/delithiation of  $\text{S}_{2-4}$  occurred as a solid-solid process, since the carbon micropore blocked the entry of solvent molecules [53]. In the recent work of Guo's group, they successively reveal novel electrochemistry versus Li of S chains encapsulated in single/double-walled carbon nanotubes and Se chains in carbon slit pores (Fig. 3b and c) [26,54]. Both studies, from either the experimental side or the theoretical side, confirm irreversible

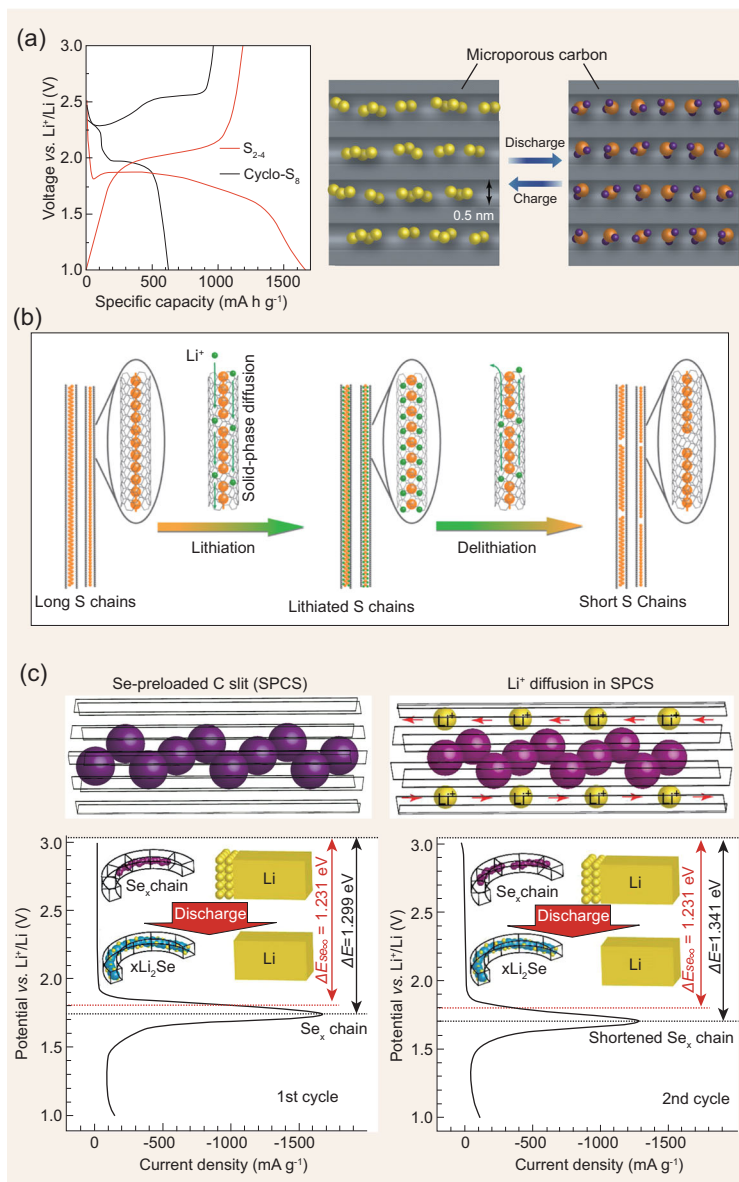


**Figure 3.** Electrochemistry versus Li of (a) small  $S_{2-4}$  allotropes confined in a microporous carbon, (b) a S chain encapsulated in a carbon nanotube and (c) a Se chain confined in a carbon slitpore. Reproduced with permission from [21] (copyright 2012, American Chemical Society), [26] (copyright 2015, American Chemical Society) and [54] (copyright 2016, American Chemical Society).

conversions from long chains to short chains of S/Se via chain shortening during initial Li intercalation (Fig. 3b and c) [26,54]. After the conversions, significantly improved electrochemical activity and stability of S/Se are observed in the subsequent cycles, which strongly prove the feasibility of using short S chains to construct high-energy cathodes [26,54]. The discovery of the novel electrochemistry of S/Se supplements the existing knowledge of the S cathode and provides new approaches for rational design of S cathode materials.

### Sulfide electrochemistry

Since M.S. Whittingham proposed the  $Li^+$  intercalation mechanism in layered titanium disulfide ( $TiS_2$ ) in the 1970 s, sulfides have been widely investigated as cathode materials for Li–S batteries [12,55]. Among these candidates,  $Li_2S$ , the end discharge product of S, is promising, since it delivers a specific capacity of 1166 mA h/g through the same electrochemistry of S versus Li yet provides a reverse direction of reaction, and enables the use of a lithium-free anode such as graphite, silicon or tin [12,15,56,57]. However, a number of challenges should be addressed before the practical cathode use of  $Li_2S$ , e.g. poor electronic/ionic conduction, sensitivity to moisture and limited preparation methods [12,15]. Targeted at the conductivity and synthesis problems of  $Li_2S$ , Manthiram's group proposes a combination use of dissolved polysulfide catholyte with porous current collector as cathode [58,59]. By dissolving the starting materials, S and  $Li_2S$ , into ether solvents, the catholyte is easily prepared and uniformly penetrated into the porous current collector to trigger better electrical contact of active S with the current collector [58,59]. Also, this strategy enables higher loading of active S than the conventional cathodes by coating S on a flat current collector [15].

Organic sulfide materials are also being studied as potential cathode materials for Li–S batteries. Wang *et al.* have proposed a sulfur–poly(acrylonitrile) composite material by introducing S in forms of thioamide and polysulfide into a poly(acrylonitrile)-derived conductive backbone [60–63]. The sulfide material shows an electrochemical behavior similar to that of small S allotropes, while also delivering a high specific capacity and stable cycling performance in various types of electrolytes including the carbonate and gel electrolytes [61–63]. In case a higher S content is realized in such a sulfide material, a prospect will be seen for its practical use for high-energy Li–S batteries.

### Strategies to improve lithium electrochemistry

As another crucial component for Li–S batteries, Li metal has been regarded as one of the most ideal anodes in rechargeable lithium batteries owing to its high theoretical capacity (3860 mA h/g) and low  $Li^+/Li$  redox potential [12,18,60]. However, unstable electrochemistry at the Li–electrolyte interface brings serious safety issues that hinder the practical anode use of Li [12,18,60]. The first problem comes with the dendrite growth on the anode surface during repeated Li plating/stripping, which leads to a low Coulombic efficiency and brings safety

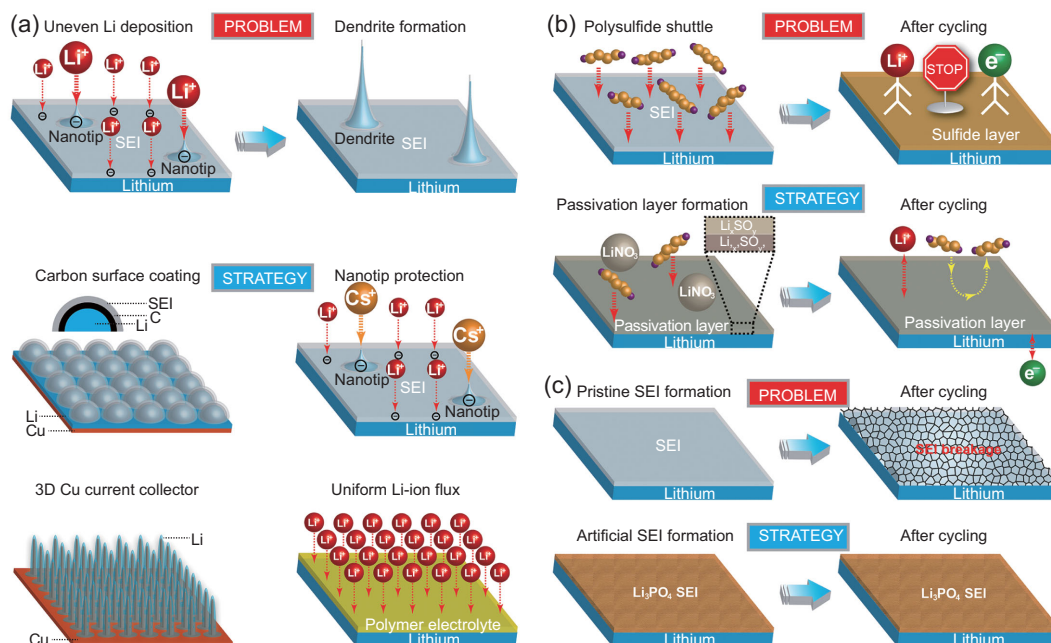


**Figure 4.** Summary of strategies to improve the electrochemistry of Li anodes: (a) strategies to prevent the dendrite formation, (b) strategy to prevent the formation of inactive sulfide layer and (c) strategy to prevent SEI breakage.

concerns, since the dendrite may penetrate through the separator. Unfortunately, it is almost impossible to eliminate the dendrite growth, since it originates from a preferential Li deposition on nano-sized tips and protruding parts of the anode surface [12,18]. Protective coating on the Li anode surface with various kinds of materials such as nanosized carbon architectures have been reported with a favorable dendrite suppression effect by physically applying pressure against the anode surface and blocking up the space for dendrite growth (Fig. 4a) [64–66]. Other methods, such as the addition of  $\text{Cs}^+$  ions at low concentrations to repel  $\text{Li}^+$  from sharp nanotips, were also reported as effective in preventing dendrite growth (Fig. 4a) [67]. Recently, Yang *et al.* proposed a new strategy to suppress the dendrite formation by plating Li into a 3D copper current collector with a submicron skeleton and high electroactive surface area (Fig. 4a) [68]. During cycling, Li grows on the submicron-sized Cu skeleton and fills the pores of the current collector without any growth outside [68]. With the Li dendrite growth being effectively suppressed, the Li anode with such a 3D current collector architecture is able to survive for 600 h without any short circuit and exhibits low voltage hysteresis to benefit its battery application [68].

A uniform Li-ion flux is the other key factor for dendrite suppression, since it prevents excessive concentration of  $\text{Li}^+$  at local domains. To ensure the uniformity of  $\text{Li}^+$  flux, the electrolyte should have a good wettability on the anode surface. For exam-

ple, in recent work by Goodenough's group, a cross-linked polymer layer was introduced between the Li anode and the electrolyte, which effectively wets the Li metal surface and homogenizes the Li-ion flux at the interface (Fig. 4a) [69]. With such a polymer interlayer, the Li anode shows a much improved electrochemical stability and a higher plating/stripping efficiency to trigger an extended cycle life [69].

Though the polysulfide shuttle in Li–S batteries brings deteriorated electrode performance, it also has optimistic sides [40,70]. According to Li *et al.*, the shuttled polysulfides can react with newly formed Li dendrite on the anode surface, so that the dendrite formation is significantly suppressed in Li–S batteries [70]. Moreover, by employing both lithium polysulfide and  $\text{LiNO}_3$  as additives in ether-based electrolyte, a uniform solid electrolyte interface is formed on the Li anode surface, so that one can synergistically prevent dendrite growth and electrolyte decomposition [70].

Another critical problem of Li anodes lies in the formation of a solid electrolyte interface (SEI). Since the Fermi level of Li is higher than the LUMO of most electrolytes, a reduction of electrolyte on the surface of Li is ineluctable (Fig. 1) [71]. Unfortunately, the SEI formation on the Li anode is not stable compared with that on the graphite or silicon [18]. The Li plating/stripping process is usually accompanied by a repeated breakage/repair of the surface SEI, which continuously consumes both Li metal and electrolyte and finally results in a low

Coulombic efficiency of the batteries. With the polysulfides shuttling to the surface of Li, the formation of the anode SEI in a Li–S battery becomes even more complicated. A sulfide layer with poor conductivity is usually formed on the surface of the Li, which hinders the Li plating/stripping and leads to deteriorated performance of the anode (Fig. 4b) [12,15]. Therefore, it is necessary to protect the anode from polysulfides and stabilize its electrochemistry.  $\text{LiNO}_3$  is commonly employed for anode protection, as it can oxidize polysulfides to  $\text{Li}_x\text{SO}_y$  moieties and be reduced by Li to  $\text{Li}_x\text{NO}_y$  species, forming a double-layer passivation top on the Li anode [40,72]. In this way, the polysulfide deposition on the Li anode is effectively suppressed (Fig. 4b). Nevertheless, the  $\text{LiNO}_3$  additive suffers from progressive consumption by continuously formed lithium dendrites and polysulfides, which is not good for the long-term operation of the battery [73,74]. Additionally,  $\text{LiNO}_3$  could be irreversibly reduced on the cathode at  $< 1.6$  V (versus  $\text{Li}^+/\text{Li}$ ), which narrows down the electrochemical window of the Li–S battery with the possible sacrifice of cathode capacity [73,74]. Therefore, new additives with strong passivation effects and stable electrochemistry are highly desired.

Recently, artificial SEI on the Li anode has been proved as a feasible strategy for stabilizing the Li electrochemistry. For example, Li *et al.* propose to build an integral  $\text{Li}_3\text{PO}_4$  SEI layer with high Young's modulus on Li via an *in situ* chemical process (Fig. 4c) [75]. The  $\text{Li}_3\text{PO}_4$  SEI layer exhibits excellent chemical stability during the Li deposition/dissolution process without any breakage, so that it effectively restrains the growth of Li dendrite and reduces the side reaction between Li and electrolytes (Fig. 4c) [75]. The strategy of building artificial SEI has demonstrated its success by enabling 200 stable cycles of Li–LiFePO<sub>4</sub> batteries. By adjusting the chemical composition and other parameters of the SEI, a prospect of artificial SEI in Li–S batteries is foreseen.

## Summary and outlook

The Li–S conversion reaction powers one of the key enabling 'post-lithium' technologies and it is good to see that the effort has led to satisfactory advancements in Li–S batteries in recent years. However, many critical problems still need to be addressed, and a deep understanding of fundamental Li–S electrochemistry may help. Moreover, given the chemical similarities of elements in Groups IA and VIA, one may want to extend his knowledge to novel conversion-type electrochemical systems,

such as Na–S, K–S, Li/Na–Se and Li/Na–Te batteries with potentially high energy output [54,76–81]. Traditional Na–S batteries employing sodium  $\beta$ -alumina as the electrolyte require a temperature of 300–350°C to operate and may bring safety concerns, since the temperature far exceeds the melting points of Na (98°C) and S (115°C). In recent work by Guo's group, they successfully demonstrated a room-temperature cyclable Na–S battery with the use of small  $\text{S}_{2-4}$  molecules as cathodes [76]. Benefiting from a high electroactivity and stable electrochemistry versus Na, the  $\text{S}_{2-4}$  cathode displays a high specific capacity, tripling that of the S cathode in a high-temperature Na–S battery, as well as a long cycle life and favorable high-rate capability [76]. In this way, a high-energy room-temperature Na–S battery is realized with a significant reduction in the operation temperature to enhance its safety [76]. Although the use of Se/Te as a cathode material may involve concerns on abundance and cost, we do believe that these new battery systems still have their place in the future market [54,77–81]. For example, Se cathode has been confirmed to hold a comparable theoretical volumetric capacity density (3250 mA h/cm<sup>3</sup>) with that of S (3470 mA h/cm<sup>3</sup>) in its reaction with Li/Na, along with a much higher electronic conductivity and more stable electrochemistry than S [54,78,81]. Thus, Li/Na–Se batteries are expected to yield equivalent volumetric energy densities to those of the Li/Na–S batteries, yet are provided with improved battery performance, making them attractive candidates for top-level storage applications where the energy density (or packing space) is the first priority (such as in spacecrafts) [54,78,81]. Moreover, considering the low cost of the Na anode, the cost inferiority of Se/Te cathodes may be offset, so that the Na–Se/Te batteries may have better economic sustainability [54]. We do believe, in an optimistic way, that joint success will consequently promote the development of next-generation rechargeable Li batteries.

## LITHIUM–OXYGEN BATTERY

### Introduction to the lithium–oxygen battery

Nowadays, the energy-storage system is believed to play an important role in our daily lives. However, traditional energy-storage systems, especially the Li-ion battery, are growing to be incapable to meet the growing energy demands from our society in the future due to their intrinsic low energy density. In response, powerful energy-storage systems with high energy density should be developed. Encouragingly, the emergence of Li–O<sub>2</sub> technology,

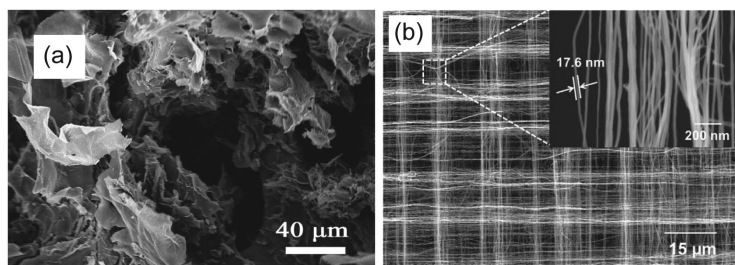


**Figure 5.** Scanning electron microscopic (SEM) images of (a) porous carbon cathodes and (b) CNT fibril (inset: large area image of the air electrode). Reproduced with permission from [97] and [98] (copyright 2012 and 2013, Wiley-VCH).

featuring the ultrahigh theoretical energy density that is 5–10 times that of the Li-ion battery [82], is a revolutionary event in the energy-storage field. As witnessed over the past decade, intensive research efforts have been devoted to Li–O<sub>2</sub> technology, which has been followed by encouraging results in the electrolyte, cathode and anode field, etc. [83–87]. Despite the breakthroughs achieved in the Li–O<sub>2</sub> field, one important thing of note is that the development of this promising Li–O<sub>2</sub> technology is still in its infancy. To make the Li–O<sub>2</sub> battery suitable for practical application, significant efforts in a variety of fields to unlock its full potential are required. Among these fields, the promotion of desirable reactions and suppression of parasitic reactions during the operation of a non-aqueous Li–O<sub>2</sub> battery is a topic of strategic importance.

In a non-aqueous Li–O<sub>2</sub> battery, the desirable reactions are related to the formation/decomposition of Li<sub>2</sub>O<sub>2</sub>, which includes a series of intermediate reactions, such as the reduction of O<sub>2</sub> on the cathode, the formation of LiO<sub>2</sub> and the release of O<sub>2</sub>, etc. [85]. And the parasitic reactions can be summarized as the corrosion of cell components covering anodes, cathodes and electrolytes in the harshly oxidative environment during the operation of Li–O<sub>2</sub> batteries [88]. It should be noted that the existence of side products generated from parasitic reactions can deteriorate the electrochemical performance of Li–O<sub>2</sub> batteries seriously [89]. Based on the previous reports, to obtain a Li–O<sub>2</sub> battery with high performance, the desirable reactions should be facilitated while the parasitic reactions need to be suppressed.

To date, many insightful reviews on Li–O<sub>2</sub> batteries have been published from various perspectives [88,90,91], which is an excellent starting point for any researchers with the desire to explore Li–O<sub>2</sub> technology. However, there are few focused on the theme of promoting desirable reactions and suppressing parasitic reactions. Therefore, to fill in the knowledge gap and provide guidance for further relevant research, this section concentrates on the recent progress in desirable reactions promotion and

parasitic reactions suppression, which will be described separately in the following parts.

## Desirable reactions promotion

A typical Li–O<sub>2</sub> battery is composed of a Li metal negative electrode, a non-aqueous electrolyte and a porous positive electrode. During discharge, O<sub>2</sub> is reduced and combines with Li<sup>+</sup> to generate insoluble discharge products (typically Li<sub>2</sub>O<sub>2</sub>) that fill up the porous electrode [89]. During charge, the generated products are decomposed with the evolution of O<sub>2</sub>. In the following sections, relevant achievements in promoting the formation/oxidation of Li<sub>2</sub>O<sub>2</sub>, the reactions of which can be called as desirable reactions in the Li–O<sub>2</sub> battery, will be discussed.

As reported, during the operation of a Li–O<sub>2</sub> battery, the formation/decomposition of Li<sub>2</sub>O<sub>2</sub> involves the mass transport of all reactants, such as dissolved oxygen, Li<sup>+</sup> and the deposition of solid Li<sub>2</sub>O<sub>2</sub> on the cathode, which can be affected by the morphology of the cathode to a great extent [92,93]. To promote these reactions, an advanced cathode with sophisticated architecture is necessary. In these aspects, various nanostructured air electrodes with smart design have been reported [94–96]. As a typical example [97], Wang *et al.* reported the synthesis of a hierarchical porous carbon cathode with nickel foam as the skeleton. Unexpectedly, the Li–O<sub>2</sub> battery with the cathode manifests a high specific capacity and an excellent rate capability. This promising performance is attributed to enough void volume, which is provided by the loose packing of the carbon in the free-standing structure, for Li<sub>2</sub>O<sub>2</sub> deposition. Meanwhile, the hierarchically porous structure, including macropores from the nickel foam, and mesopores and micropores from the carbon particles, facilitates mass transport of all the reactants and wetting of the electrolyte (Fig. 5a). In another work [98], Lim has reported the construction of a hierarchical porous electrode with a controlled porous framework achieved by orthogonally plying sheets of well-aligned multiwalled nanotubes (MWNTs) on the Ni-mesh current collector as a whole part (Fig. 5b). Benefiting from the easy access of oxygen to the inner space of the electrode and sufficient room for Li<sub>2</sub>O<sub>2</sub> deposition, the woven fibrils electrode has exhibited a notable cycling stability for 100 cycles and an excellent rate capacity for 60 cycles at a current rate of 1000 mA/g.

In addition to the promoted mass transfer of all reactants and Li<sub>2</sub>O<sub>2</sub> deposition, the decomposition of Li<sub>2</sub>O<sub>2</sub> is another important aspect that cannot be ignored, given its direct relevance to the electrochemical performance of the Li–O<sub>2</sub> battery, such

as round-tip efficiency and Coulombic efficiency [92,99]. Even though the construction of the cathode with advanced architecture can facilitate the mass transfer of all reactants, the insufficient oxygen evolution reaction (OER) activity of these pure carbon materials has restricted their application in the Li–O<sub>2</sub> battery. As a remedy, the incorporation of an OER effective catalyst is a choice of great promise. To date, a tremendous amount of effort has been devoted to exploring effective catalysts to promote the OER kinetics in Li–O<sub>2</sub> batteries. Various types of materials, including metals [100], metal oxides [101] and transition bimetallic nitrides [102], have been investigated. Among these materials, perovskite-based oxides, which hold many favorable physical/chemical properties including high electronic/ionic conductivity, high electrochemical stability and enhanced catalytic characteristics [103], are promising candidates as electrocatalysts for Li–O<sub>2</sub> batteries. As reported by Xu [82], perovskite-based porous La<sub>0.75</sub>Sr<sub>0.25</sub>MnO<sub>3</sub> nanotubes (PNT-LSM) via an electrospinning technique and subsequent heating treatment were developed. When this catalyst is employed as the electrocatalyst in a Li–O<sub>2</sub> battery, the decomposition of Li<sub>2</sub>O<sub>2</sub> is effectively promoted and the round-trip efficiency is effectively improved. In another typical example [104], Oh reported the utilization of metallic pyrochlore as a catalyst that exhibits a lower charge potential for Li<sub>2</sub>O<sub>2</sub> oxidation than pure carbon. The enhanced Li–O<sub>2</sub> charging efficiency was ascribed to the increased mass transport of reaction intermediate species that is promoted by both the high oxygen vacancies and the porosity of the pyrochlore, thereby providing guidance for new catalyst designs in the Li–O<sub>2</sub> cell. In parallel importance with OER kinetic promotion during charge, the charge transfer in oxidizing Li<sub>2</sub>O<sub>2</sub> needs to be accelerated as well, given the fact that a slow charge transfer can lead to a much higher charge voltage [103]. In light of previous reports, the kinetics of the charge transfer can be significantly affected by the Li<sub>2</sub>O<sub>2</sub> coverage region on the cathode due to the preferential oxidation of electrochemically formed Li<sub>2</sub>O<sub>2</sub> particles at the carbon/Li<sub>2</sub>O<sub>2</sub> interface during charge [105]. Therefore, it is feasible to facilitate the charge transfer with a maximized carbon/Li<sub>2</sub>O<sub>2</sub> interfacial area. In response, the morphology and distribution of the generated Li<sub>2</sub>O<sub>2</sub> rather than the traditionally produced Li<sub>2</sub>O<sub>2</sub> that is featured with a toroidal morphology and sparse distribution around the carbon cathode should be optimized [106]. In response, the surface electronic state of the cathode materials needs to be tuned, since the formation of Li<sub>2</sub>O<sub>2</sub> is an electron-induced process [107]. Recently, through wet impregnation and subsequent thermal annealing treat-

ment, a hybrid of a carbon nanotube-encapsulated noble metal nanoparticle (Pd, Pt, Ru and Au) has been developed [108]. Of note in the study is that, by strengthening the electron density on the carbon nanotube (CNT) cathode surface with the confinement of ‘guest’ nanoparticles (NPs) inside the ‘host’ CNTs, which has avoided the local enrichment of the electron density resulting from the direct exposure of NPs on the CNT surface, the nucleation of Li<sub>2</sub>O<sub>2</sub> is promoted around the entire NPs-encapsulated CNTs surfaces, contrasting with that on the NPs-supported CNTs surface (Fig. 6a and d). Therefore, a uniform coverage of Li<sub>2</sub>O<sub>2</sub> nanocrystals on NPs-encapsulated CNT surfaces rather than the localized distribution of Li<sub>2</sub>O<sub>2</sub> aggregation on NPs-supported CNTs surfaces is favored, which has more effectively facilitated the charge transfer for the electrochemically oxidation of Li<sub>2</sub>O<sub>2</sub> (Fig. 6b and e). On this account, the cathode materials with NPs encapsulated on the CNTs surface demonstrate a much lower charge voltage than their counterparts with NPs anchored on the CNT surface (Fig. 6c and f). In addition to the morphology of Li<sub>2</sub>O<sub>2</sub> and its distribution on the cathode, the degree of crystallinity of the deposited Li<sub>2</sub>O<sub>2</sub> is another important factor in influencing the charge transfer [109]. On the basis of previous discoveries, amorphous Li<sub>2</sub>O<sub>2</sub> possesses more conductivity than the crystalline one, which is suggested to promote the smooth decomposition of Li<sub>2</sub>O<sub>2</sub> during the charge process, thus translating to a low charge overpotential [110]. In this regard, the discharge mechanism should be biased by tuning the electrochemical environment of the cathode with the incorporated catalyst. Recently, Yilmaz *et al.* reported the promoted formation of noncrystalline Li<sub>2</sub>O<sub>2</sub> with RuO<sub>2</sub> NPs deposited on the multi-walled CNTs (MWCNTs) cathode [111], resulting from the stronger oxygen-adsorption energy on the RuO<sub>2</sub> NPs than that on the MWCNTs. Notably, besides the large coverage region provided by the shapeless Li<sub>2</sub>O<sub>2</sub> deposited on the RuO<sub>2</sub>/CNT cathode, the higher conductivity of this unique Li<sub>2</sub>O<sub>2</sub> structure associated with defects further promotes its smooth decomposition at low charge potential, contrasting sharply with the crystalline Li<sub>2</sub>O<sub>2</sub> formed on the pure MWCNTs (Fig. 6g–i).

Taken together, the significance of improvement, which the catalysts provide over the ORR/OER pathways, on promoting Li<sub>2</sub>O<sub>2</sub> decomposition is quite obvious. However, it should be noted that this kind of oxidation only happens at the limited and rigid contact surface between the cathode and deposited Li<sub>2</sub>O<sub>2</sub> [105], leading to severe polarization in most cases. What is worse, the existence of an incorporated catalyst, whose mass density is larger than that of carbon, is expected to increase

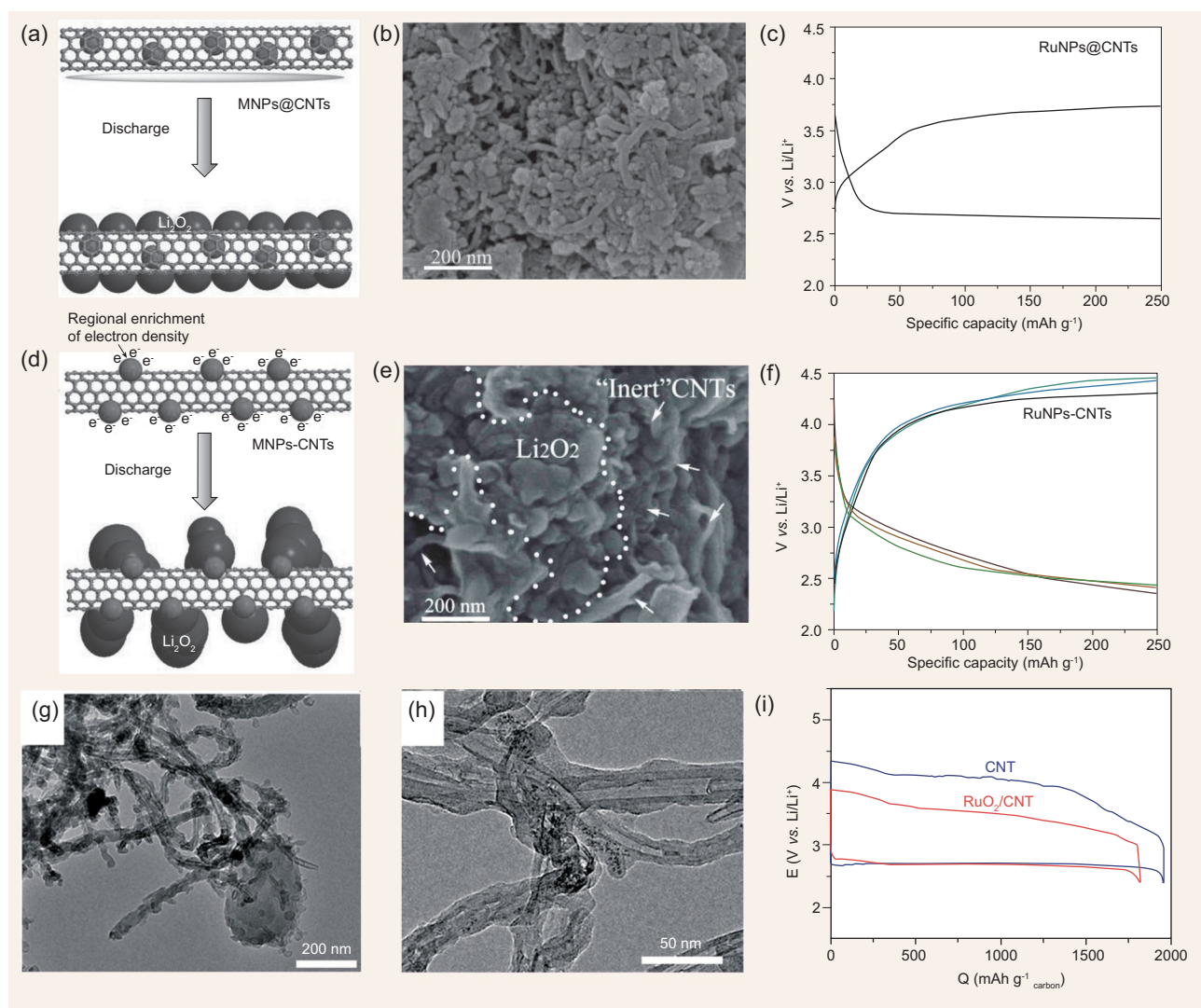


**Figure 6.** Proposed mechanism for the nucleation of Li<sub>2</sub>O<sub>2</sub> on the (a) MNPs@CNT cathode and (d) MNPs-CNT cathode after the 10th discharge. SEM images of the (b) Ru@CNT cathode and (e) Ru-CNTs cathode after the 10th discharge. Cycling performances of the (c) Ru@CNT cathode and (f) Ru NPs-CNTs cathode. SEM images of the discharged (g) CNT cathode and (h) RuO<sub>2</sub>/CNT cathode. (i) The initial discharge-charge performances of the CNT and RuO<sub>2</sub>/CNT cathode at a current density of 0.05 mA/cm<sup>2</sup> with a cut-off discharge voltage of 2.4 V. Reproduced with permission from [108] (copyright 2014, Wiley-VCH) and [111] (copyright 2013, American Chemical Society).

the weight of the whole electrode. As a result, the mass energy density of the Li-O<sub>2</sub> battery is compromised and the practical application of the Li-O<sub>2</sub> battery is restricted. To counter these problems, the injection of redox mediators (RM) into the electrolyte is an approach of great promise. As reported, during charge, the dissolved RM can act as mobile charge carriers between the electrode surface and deposited Li<sub>2</sub>O<sub>2</sub>. The charge transfer is based on the reversible redox pair  $RM \rightleftharpoons RM^+ + e^-$ . As a benefit, the generated Li<sub>2</sub>O<sub>2</sub> can be effectively oxidized thanks to the much larger and dynamic interphase between Li<sub>2</sub>O<sub>2</sub> and the liquid electrolyte, thus realizing a much reduced charge overpotential. In pioneering work by Bruce [112], a redox-mediating

molecule (TTF) is incorporated into the electrolyte for the rechargeable non-aqueous Li-O<sub>2</sub> battery and demonstrates an efficient oxidation of Li<sub>2</sub>O<sub>2</sub>. Notably, with the help of TTF, the Li-O<sub>2</sub> battery can be recharged at a current density (1 mA/cm<sup>2</sup>) that is impossible without the redox mediator in the same cell. Simultaneously, the cell with the mediator demonstrates 100 charge/discharge cycles at such high current density. After this, a similar research on reducing the charge potential was carried out by Kisuk Kang [113]. In this research, a new redox mediator LiI was applied, which has demonstrated excellent ability in decomposing Li<sub>2</sub>O<sub>2</sub> as well. To a certain degree, the achievement by the two pieces of research on reducing the charge

overpotential has ignited a growing interest in the redox mediator field. The last three years have witnessed a surging interest in the research of RM [114–116]. Among them, a nitroxide compound TEMPO (2,2,6,6-tetramethylpiperidinyloxy) with favorable properties for the OER in Li–O<sub>2</sub> cells is proposed [114]. Compared with the Li–O<sub>2</sub> battery without TEMPO, a reduction of 500 mV in the charging potential is realized in the Li–O<sub>2</sub> battery with TEMPO. In other research by Sun [115], iron phthalocyanine (FePc) is applied as a shuttle of (O<sub>2</sub>)<sup>−</sup> species and electrons between the surface of the electronic conductor and the insulator Li<sub>2</sub>O<sub>2</sub> product of discharge. The Li<sub>2</sub>O<sub>2</sub> is observed to grow and decompose without direct contact with carbon, which greatly enhances the electrochemical performance. Impressively, the charge potential of Li–O<sub>2</sub> batteries with FePc is much lower than without FePc. What is more, the Li–O<sub>2</sub> battery with FePc also exhibits a greater prolonged cycling stability than that without FePc.

In summary, the strategies mentioned above have promoted the desirable reaction to a varying degree. Despite these achievements, it should be noted that more research efforts are necessary towards the final practical application of the Li–O<sub>2</sub> battery.

### Parasitic reactions suppression

As electrochemical energy-storage technology with the highest theoretical capacity, lithium–oxygen batteries face critical challenges in terms of poor stabilities and low charge/discharge round-trip efficiencies. It is generally recognized that these issues are connected to the parasitic chemical reactions at the anode, electrolyte and cathode, which will be summarized and discussed separately in the following section along with relevant achievements in parasitic reactions suppression.

Metallic lithium is the current choice for the metal electrode material for Li–O<sub>2</sub> batteries, which is expected to achieve the highest energy density at the cell level, since lithium itself has an extremely high specific energy (3860 mA h/g) and a low negative potential (−3.04 V versus standard hydrogen electrode, SHE) [91]. The desired reactions at the Li anode are the stripping (during discharge) and plating (during charge) of lithium [88]. But the high reactivity and low redox potential of Li dictate that complex chemical reactions often take place when Li is in contact with other chemicals [117]. As reported by Shui [118], metallic lithium can be converted into LiOH on the anode until the complete consumption of the Li metal, which is detrimental to the cycling stability of the Li–O<sub>2</sub> battery. Simultaneously, the undesirable growth of dendrital lithium on the Li

metal anode surface upon cycling would inevitably cause serious safety problems. In response, a few approaches to suppress these reactions on the pristine Li anode in Li–O<sub>2</sub> batteries have been reported [116–123], including using special electrolyte and additive, coating a protective polymer layer, soaking with organic solvent, and even replacing Li anode with low-potential and high-capacity silicon alloy anode material. To be specific, in the research by Wallker [119], a stable SEI is formed on the Li anode with the use of N,N-dimethylacetamide (DMA) dissolving LiNO<sub>3</sub>, thus enabling a prolonged cycling of the Li anode.

Although these strategies alleviate Li corrosion to some extent, they are still far from satisfying in terms of the high cost requirement and the complex treatment process, instability of the formed protection film and especially when further considering the fact that enhancement in the cycle life of Li–O<sub>2</sub> batteries is still very limited. Therefore, the development of a novel strategy to effectively protect the Li metal anode to significantly improve the cycle stability of Li–O<sub>2</sub> batteries is highly desirable yet still very challenging. In this aspect, Liu *et al.* have proposed and realized a facile while very effective strategy to protect the Li anode [124], which is achieved by artificially fabricating a protection film on the metal Li. In this research, the protective film is formed by charging a symmetric Li/electrolyte/Li cell. Notably, the as-obtained protected lithium anode endows the Li–O<sub>2</sub> battery with superior cycle stability—more than 100 stable cycles, which is more than three times that of the Li–O<sub>2</sub> battery with the pristine Li metal as an anode (31 cycles). This significant enhancement of the cycling stability could be attributed to the artificial protective film, which effectively protects the Li metal from corroding of organic solvent and dissolved O<sub>2</sub> during discharge–charge cycles.

In the lithium–oxygen battery, a porous carbon material is widely chosen as the cathode material, benefiting from good properties such as its being lightweight, environmentally benign, cost-effective and with good conductivity. Despite being so, the problems from the parasitic reactions, which are caused by the chemical instability of the carbonaceous material in the oxidative environment of the Li–O<sub>2</sub> battery, have restricted its application in the Li–O<sub>2</sub> field. In light of previous reports, during the operation of the Li–O<sub>2</sub> battery, oxidation of the carbon by Li<sub>2</sub>O<sub>2</sub> or other reaction intermediates to Li<sub>2</sub>CO<sub>3</sub>-like species can occur [125]. As a result, the build-up of these species deactivates the active sites on the carbon cathode and hinders charge transfer essential for oxygen evolution [91], therefore leading to an increase in the overpotential during subsequent charge processes. Clearly, to obtain a Li–O<sub>2</sub>

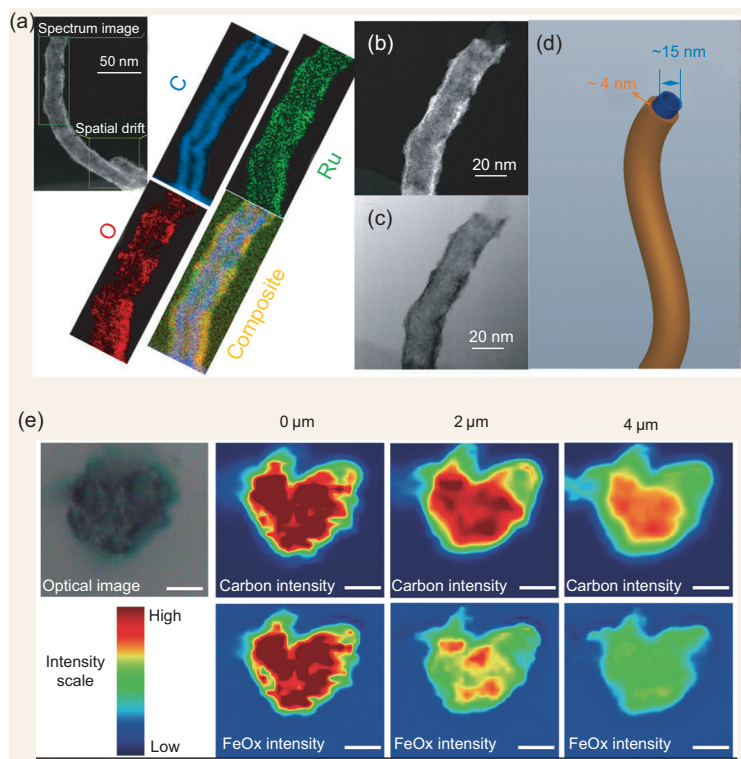


**Figure 7.** (a) The dark field (HAADF)-scanning transmission electron microscopy (STEM) image and corresponding energy-dispersive X-ray (EDX) maps of the cathode. (b) HAADF-STEM and (c) bright-field (BF) STEM images of an individual CNT@RuO<sub>2</sub> architecture. (d) Schematic illustration of the core/shell CNT@RuO<sub>2</sub> configuration. (e) Raman mapping of FeO<sub>x</sub>-coated 3D0m carbon. Top left: photographical image of the researched carbon particle. Top right panels: carbon signal mapping with different focal depth; bottom right panels: FeO<sub>x</sub> signal mapping with the same focal depths. Scale bars: 5 μm. Reproduced with permission from [126] and [127] (copyright 2014, Wiley-VCH).

battery with desirable performance, the parasitic reactions arising from the application of carbon materials need to be suppressed. To this end, the chemical stability of carbonaceous materials is required to be improved. In this aspect, Jian *et al.* reported a new cathode with high resistance to carbon corrosion [126], which is achieved by coating the CNT with a uniform RuO<sub>2</sub> layer. Upon being applied in the Li–O<sub>2</sub> battery, this new cathode has endowed the Li–O<sub>2</sub> battery with a constant specific capacity for over 100 cycles at a high current of 500 mA<sub>g<sub>total</sub></sub><sup>−1</sup> (Fig. 7a–d). In similar research by Xie *et al.* (Fig. 7e), a protective layer of FeO<sub>x</sub> was uniformly coated onto the carbon cathode surface by atomic layer deposition (ALD) that successfully concealed the carbon surface from the oxidative species [127]. As a benefit, the parasitic reactions caused by carbon instability are suppressed effectively and the protected carbon cathode demonstrates an extended cycle life compared to the bare carbon. In addition to the reactivity exhibited by carbon materials, the defects sites on the carbonaceous materials are also active with

superoxide radicals to generate undesirable products such as carbonates, thus undermining the round-trip efficiency and cycling stability of the Li–O<sub>2</sub> battery. On this account, the surface chemistry of the carbonaceous materials should be optimized with the aim to suppress the associated parasitic reactions. In this aspect, the annealing treatment on the carbonaceous materials makes sense. As reported [128], a strategy of heat treatment under argon atmosphere was carried out to reduce the amount of surface oxygen and selectively eliminate some unstable oxygen groups on the graphene cathode. Consequently, the amount of Li<sub>2</sub>CO<sub>3</sub> formed on the heated graphene cathode was much smaller than that on the pristine cathode, which was evident from the drop in the area ratio of Li<sub>2</sub>O<sub>2</sub>/Li<sub>2</sub>CO<sub>3</sub> from 3.9 to 1.6, according to the XPS results of the discharged cathodes. As a benefit, the graphene cathode with improved surface chemistry exhibited a much extended cycling stability.

Despite the recent progress in suppressing the parasitic reactions from the chemical instability of carbon materials, it should be noted that the challenges from the parasitic reactions aroused by carbon cathodes still exist. In most cases, a considerable amount of carbon material from carbon cathodes is exposed to the oxidative species. As a sound solution, the application of carbon-alternative materials with inertness under the harshly oxidative environment holds a great promise [122].

By replacing the widely used carbon cathode with a nanoporous gold (NPG) cathode [122], the problems associated with parasitic reactions from carbon materials are effectively circumvented, and an overwhelmingly reversible formation/decomposition of Li<sub>2</sub>O<sub>2</sub> for 100 cycles was constructed. Since then, numerous studies in developing carbon-alternative cathodes have been reported [122,129–134], including the construction of Ru/ITO cathodes [129], Pt-modified TiO<sub>2</sub> nanotube arrays cathodes [130], hollow RuO<sub>2</sub> cathodes [131], etc. To be specific, with the help of the template removal method, RuO<sub>2</sub> hollow spheres are successfully synthesized. After coating the Al foil with the mixture of RuO<sub>2</sub> hollow spheres and lithiated Nafion, a stable RuO<sub>2</sub> carbon-free cathode is successfully synthesized. When applied in the Li–O<sub>2</sub> battery, this stable cathode has demonstrated excellent electrochemical performance. In another report by Xie [132], a stable TiSi<sub>2</sub> nanonet rather than the carbonaceous material is applied as the cathode support. After the deposition of Ru nanoparticles with ALD, a carbon-free Ru/TiSi<sub>2</sub> cathode with high corrosion resistance to oxidative radicals is constructed. Benefiting from the stability of these materials, the parasitic reactions associated with carbon decomposition are thoroughly

suppressed. However, to realize a Li–O<sub>2</sub> battery without any parasitic reactions, more efforts are necessary. In this regard, Thotiyl *et al.* have reported the fabrication of a TiC cathode [133], which even outperforms the NPG in terms of chemical stability. Notably, the origin of the superior ability of TiC in suppressing the parasitic reactions is also probed. As unveiled, both the existence of TiOC and TiO<sub>2</sub> formed on the TiC are suggested to be responsible for the superior stability, which illustrates the prime importance of a stable interface to a stable carbon-alternative cathode. Consistently with the result from Thotiyl, Nazar reported a cathode based on metallic Magnéli phase Ti<sub>4</sub>O<sub>7</sub> [134]. It is reported that the conductive, self-passivating substoichiometric metal oxide layer formed at the surface is suggested to be responsible for the suppression of parasitic reactions occurring on the cathode during the operation of a Li–O<sub>2</sub> battery.

In Li–O<sub>2</sub> batteries, as a medium to transfer Li<sup>+</sup> ions and O<sub>2</sub> molecules and dissolve the reaction intermediates, the electrolyte also constitutes an important component of the Li–O<sub>2</sub> battery, of which the properties can affect the performances of the Li–O<sub>2</sub> battery significantly. In a similar case to the carbon materials, the parasitic reactions due to the reactions between electrolytes and the reaction intermediates have generated unwanted products, which have decayed the performance of the Li–O<sub>2</sub> battery significantly [135]. In response, numerous research efforts have been devoted to suppressing the parasitic reactions associated with electrolyte decomposition. A major achievement is the application of ether-based electrolytes rather than the conventional carbonate-based electrolytes, which can be decomposed in the presence of reduced oxygen discharge products [136]. However, to our regret, even the widely used ether-based electrolyte fails to avoid degradation during the operation of the Li–O<sub>2</sub> battery [137]. Clearly, the road is still very long before the arrival of success in completely suppressing parasitic reactions during the operation of a Li–O<sub>2</sub> battery.

### Summary and outlook

In the field of Li–O<sub>2</sub> technology, the topic of desirable reactions promotion and parasitic reactions suppression is of strategic importance given the direct correlation between these reactions and the performance of the Li–O<sub>2</sub> battery. Luckily, numerous studies have been devoted to relevant areas, accompanied by encouraging achievements. However, the challenges from desirable reactions promotion and parasitic reactions suppression still exist and more

efforts are necessary so as to obtain a Li–O<sub>2</sub> battery for practical application. For these considerations, some relevant suggestions are provided. On the one hand, the search for the construction of a stable cathode, the application of stable electrolytes and the protection of the Li anode should be continued. On the other hand, knowledge of the desirable reactions and parasitic reactions should be deepened. To this end, various *in situ* techniques should be developed, since they can explore the fundamental nanoscale processes, based on which more effective strategies in promoting the desirable reactions and suppressing the parasitic reactions can be provided.

### CONCLUSIONS

The shifted interests from intercalation compounds to conversion electrochemistry have witnessed an ongoing pursuit for advanced storage devices with higher energy densities to power modern civilization. With efforts made and progress achieved, the Li–S and Li–O<sub>2</sub> batteries have demonstrated their potentials in surpassing the current Li-ion technology. Challenges, however, still exist in the science and engineering aspects of these new electrochemical systems. It is still premature to judge their prospects on the ‘post-lithium’ market, since there is still uncertainty whether the energy density, especially the volumetric energy of practical Li–S (O<sub>2</sub>) batteries, can compete with the Li-ion battery (Fig. 8). Therefore, it is necessary to look deep into the fundamental conversion electrochemistry of S (O<sub>2</sub>) versus Li before we can reveal the operational feasibilities and limitations of batteries.

Despite a vast amount of pioneering work in the field, it is hard to incorporate all the aspects in this review. Although emphasis is placed on the key components of Li–S (O<sub>2</sub>) batteries, many other factors, such as conductive additives, binders, separators, current collectors, cases and even engineering aspects including cell encapsulation and pack design, should be considered thoroughly to yield a satisfactory product. An interdisciplinary collaboration will be helpful to develop practical Li–S and Li–O<sub>2</sub> batteries with satisfactory energy output and cycle life.

In view of a limited global source of Li, conversion-type batteries based on alternative alkali metal anode materials with richer abundances, such as Na and K, should be considered. For example, Na–S batteries and Na–O<sub>2</sub> batteries are also provided with attractive theoretical energy outputs, yet benefit from a significant reduction in anode cost [76,138]. Recent work by Goodenough’s group has proposed a new liquid K–Na alloy

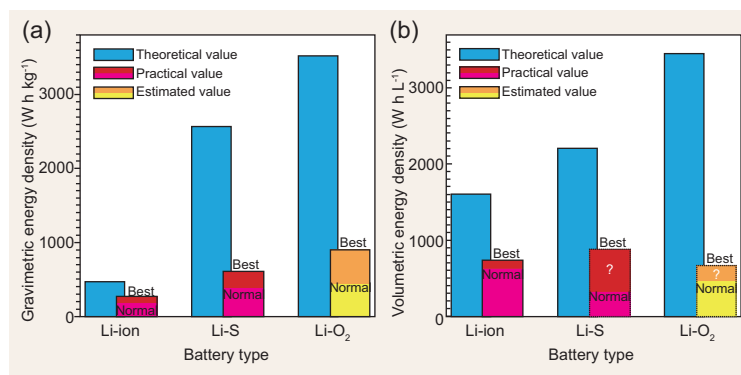


**Figure 8.** Comparison of (a) gravimetric energy densities and (b) volumetric energy densities between intercalation-type Li-ion battery and conversion-type Li-S and Li-O<sub>2</sub> batteries. A LiNi<sub>0.8</sub>Co<sub>0.15</sub>Al<sub>0.05</sub>O<sub>2</sub>-graphite battery is adopted to represent the Li-ion battery, since it holds competitive energy outputs among all the state-of-the-art Li-ion batteries. The theoretical energy densities of the Li-ion battery are calculated based on the LiNi<sub>0.8</sub>Co<sub>0.15</sub>Al<sub>0.05</sub>O<sub>2</sub> cathode and the graphite anode, and the practical values are obtained from commercial 18650-type cells. The theoretical and practical energy densities of the Li-S and Li-O<sub>2</sub> batteries are obtained from [11] and [18]. Since the Li-O<sub>2</sub> battery or its key components are not commercially available, we cannot provide a precise evaluation of its practical energy density. Therefore, only estimated values are given.

anode, which enables high-energy rechargeable K batteries free of dendrite formation [139]. Other conversion-type batteries based on anodes with multielectron-transfer ability, such as Zn-O<sub>2</sub>, Mg-S and Al-S batteries, are also promising [18,140,141]. For example, the rechargeable Zn-O<sub>2</sub> battery, although it delivers lower energy density than the Li-O<sub>2</sub> battery, is provided with decent cycling and rate performance and, more importantly, a much lower cost if operated in an aqueous electrolyte [18,142]. Hence, it may be considered as an appealing choice for future stationary storage. Though the future remains unknown, one thing becomes clear: predictable success is waiting ahead and whichever wins the next round of the energy-storage battle will contribute to better economic sustainability.

## FUNDING

This work was supported by the Ministry of Science and Technology of the People's Republic of China (2016YFA0202500, 2014CB932300), the National Natural Science Foundation of China (51225204) and the Chinese Academy of Sciences Strategic Priority Research Program (XDA09010300, XDA09010404).

*Conflict of interest statement.* None declared.

## REFERENCES

1. Armand M and Tarascon JM. Building better batteries. *Nature* 2008; **451**: 652–7.

2. Lai X, Halpert JE and Wang D. Recent advances in micro-/nano-structured hollow spheres for energy applications: from simple to complex systems. *Energy Environ Sci* 2012; **5**: 5604–18.
3. Wang J, Yang N and Tang H *et al.* Accurate control of multi-shelled Co<sub>3</sub>O<sub>4</sub> hollow microspheres as high-performance anode materials in lithium-ion batteries. *Angew Chem Int Ed* 2013; **52**: 6417–20.
4. Xu S, Hessel CM and Ren H *et al.*  $\alpha$ -Fe<sub>2</sub>O<sub>3</sub> multi-shelled hollow microspheres for lithium ion battery anodes with superior capacity and charge retention. *Energy Environ Sci* 2014; **7**: 632–7.
5. Wang J, Tang H and Zhang L *et al.* Multi-shelled metal oxides prepared via an anion-adsorption mechanism for lithium-ion batteries. *Nat Energy* 2016; **1**: 16050.
6. Qi J, Lai X and Wang J *et al.* Multi-shelled hollow micro-/nanostructures. *Chem Soc Rev* 2015; **44**: 6749–73.
7. Wang B, Chen JS and Lou XW. Quasiemulsion templated formation of  $\alpha$ -Fe<sub>2</sub>O<sub>3</sub> hollow spheres with enhanced lithium storage properties. *J Am Chem Soc* 2011; **133**: 17146–8.
8. Wang B, Wu HB and Zhang L *et al.* Self-supported construction of uniform Fe<sub>3</sub>O<sub>4</sub> hollow microspheres from nanoplate building blocks. *Angew Chem Int Ed* 2013; **52**: 416–8.
9. Wang B, Wu XL and Shu CY *et al.* Synthesis of CuO/graphene nanocomposite as a high-performance anode material for lithium-ion batteries. *J Mater Chem* 2010; **20**: 10661–4.
10. Herbert D and Ulam J. Electric dry cells and storage batteries. 1962, US patent 3,043,896.
11. Bruce PG, Freunberger SA and Hardwick LJ *et al.* Li-O<sub>2</sub> and Li-S batteries with high energy storage. *Nat Mater* 2012; **11**: 19–29.
12. Yin YX, Xin S and Guo YG *et al.* Lithium-sulfur batteries: electrochemistry, materials, and prospects. *Angew Chem Int Ed* 2013; **52**: 13186–200.
13. Ji X, Lee KT and Nazar LF. A highly ordered nanostructured carbon-sulphur cathode for lithium-sulphur batteries. *Nat Mater* 2009; **8**: 500–6.
14. Evers S and Nazar LF. New approaches for high energy density lithium-sulfur battery cathodes. *Acc Chem Res* 2013; **46**: 1135–43.
15. Manthiram A, Fu Y and Chung SH *et al.* Rechargeable lithium-sulfur batteries. *Chem Rev* 2014; **114**: 11751–87.
16. Yang Y, Zheng G and Cui Y. Nanostructured sulfur cathodes. *Chem Soc Rev* 2013; **42**: 3018–32.
17. Xin S, Guo YG and Wan LJ. Nanocarbon networks for advanced rechargeable lithium batteries. *Acc Chem Res* 2012; **45**: 1759–69.
18. Choi JW and Aurbach D. Promise and reality of post-lithium-ion batteries with high energy densities. *Nat Rev Mater* 2016; **1**: 16013.
19. Greenwood NN and Earnshaw A. *Chemistry of the Elements*. Oxford: Butterworth-Heinemann, 1997.
20. Xu DW, Xin S and You Y *et al.* Built-in carbon nanotube network inside a biomass-derived hierarchically porous carbon to enhance the performance of the sulfur cathode in a Li-S battery. *ChemNanoMat* 2016; **2**: 712–8.

21. Xin S, Gu L and Zhao NH *et al.* Smaller sulfur molecules promise better lithium–sulfur batteries. *J Am Chem Soc* 2012; **134**: 18510–3.
22. Yang CP, Yin YX and Ye H *et al.* Insight into the effect of boron doping on sulfur/carbon cathode in lithium–sulfur batteries. *ACS Appl Mater Interfaces* 2014; **6**: 8789–95.
23. Zhang J, Yang CP and Yin YX *et al.* Sulfur encapsulated in graphitic carbon nanocages for high-rate and long-cycle lithium–sulfur batteries. *Adv Mater* 2016; **28**: 9539–44.
24. You Y, Zeng W and Yin YX *et al.* Hierarchically micro/mesoporous activated graphene with a large surface area for high sulfur loading in Li–S batteries. *J Mater Chem A* 2015; **3**: 4799–802.
25. Du WC, Yin YX and Zeng XX *et al.* Wet chemistry synthesis of multidimensional nanocarbon–sulfur hybrid materials with ultrahigh sulfur loading for lithium–sulfur batteries. *ACS Appl Mater Interfaces* 2016; **8**: 3584–90.
26. Yang CP, Yin YX and Guo YG *et al.* Electrochemical (de)lithiation of 1D sulfur chains in Li–S batteries: a model system study. *J Am Chem Soc* 2015; **137**: 2215–8.
27. Du XL, You Y and Yan Y *et al.* Conductive carbon network inside a sulfur-impregnated carbon sponge: a bioinspired high-performance cathode for Li–S battery. *ACS Appl Mater Interfaces* 2016; **8**: 22261–9.
28. Pang Q and Nazar LF. Long-life and high-areal-capacity Li–S batteries enabled by a light-weight polar host with intrinsic polysulfide adsorption. *ACS Nano* 2016; **10**: 4111–8.
29. Song J, Xu T and Gordin ML *et al.* Nitrogen-doped mesoporous carbon promoted chemical adsorption of sulfur and fabrication of high-areal-capacity sulfur cathode with exceptional cycling stability for lithium–sulfur batteries. *Adv Funct Mater* 2014; **24**: 1243–50.
30. Zhou W, Guo B and Gao H *et al.* Low-cost higher loading of a sulfur cathode. *Adv Energy Mater* 2016; **6**: 1502059.
31. Wei Seh Z, Li W and Cha JJ *et al.* Sulphur–TiO<sub>2</sub> yolk–shell nanoarchitecture with internal void space for long-cycle lithium–sulphur batteries. *Nat Commun* 2013; **4**: 1331.
32. Liang X, Hart C and Pang Q *et al.* A highly efficient polysulfide mediator for lithium–sulfur batteries. *Nat Commun* 2015; **6**: 5682.
33. Fan CY, Xiao P and Li HH *et al.* Nanoscale polysulfides reactors achieved by chemical Au–S interaction: improving the performance of Li–S batteries on the electrode level. *ACS Appl Mater Interfaces* 2015; **7**: 27959–67.
34. Tao X, Wang J and Liu C *et al.* Balancing surface adsorption and diffusion of lithium–polysulfides on nonconductive oxides for lithium–sulfur battery design. *Nat Commun* 2016; **7**: 11203.
35. Yang Y, Yu G and Cha JJ *et al.* Improving the performance of lithium–sulfur batteries by conductive polymer coating. *ACS Nano* 2011; **5**: 9187–93.
36. Zhou W, Wang C and Zhang Q *et al.* Tailoring pore size of nitrogen-doped hollow carbon nanospheres for confining sulfur in lithium–sulfur batteries. *Adv Energy Mater* 2015; **5**: 1401752.
37. Zhang C, Wu HB and Yuan C *et al.* Confining sulfur in double-shelled hollow carbon spheres for lithium–sulfur batteries. *Angew Chem Int Ed* 2012; **51**: 9592–5.
38. Gao J, Lowe MA and Kiya Y *et al.* Effects of liquid electrolytes on the charge–discharge performance of rechargeable lithium/sulfur batteries: electrochemical and in-situ X-ray absorption spectroscopic studies. *J Phys Chem C* 2011; **115**: 25132–7.
39. Markevich E, Salitra G and Rosenman A *et al.* Fluoroethylene carbonate as an important component in organic carbonate electrolyte solutions for lithium sulfur batteries. *Electrochem Commun* 2015; **60**: 42–6.
40. Aurbach D, Pollak E and Elazari R *et al.* On the surface chemical aspects of very high energy density, rechargeable Li–sulfur batteries. *J Electrochem Soc* 2009; **156**: A694–702.
41. Armand M, Endres F and MacFarlane DR *et al.* Ionic–liquid materials for the electrochemical challenges of the future. *Nat Mater* 2009; **8**: 621–9.
42. Ji L, Rao M and Zheng H *et al.* Graphene oxide as a sulfur immobilizer in high performance lithium/sulfur cells. *J Am Chem Soc* 2011; **133**: 18522–5.
43. Han F, Yue J and Fan X *et al.* High-performance all-solid-state lithium–sulfur battery enabled by a mixed-conductive Li<sub>2</sub>S nanocomposite. *Nano Lett* 2016; **16**: 4521–7.
44. Suo L, Hu YS and Li H *et al.* A new class of solvent-in-salt electrolyte for high-energy rechargeable metallic lithium batteries. *Nat Commun* 2013; **4**: 1481.
45. Bai S, Liu X and Zhu K *et al.* Metal–organic framework-based separator for lithium–sulfur batteries. *Nat Energy* 2016; **1**: 16094.
46. Su YS, Fu Y and Cocheil T *et al.* A strategic approach to recharging lithium–sulphur batteries for long cycle life. *Nat Commun* 2013; **4**: 2985.
47. Su YS and Manthiram A. Lithium–sulphur batteries with a microporous carbon paper as a bifunctional interlayer. *Nat Commun* 2012; **3**: 1166.
48. Chung SH and Manthiram A. A natural carbonized leaf as polysulfide diffusion inhibitor for high-performance lithium–sulfur battery cells. *ChemSusChem* 2014; **7**: 1655–61.
49. Ryu HS, Ahn HJ and Kim KW *et al.* Self-discharge characteristics of lithium/sulfur batteries using TEGDME liquid electrolyte. *Electrochim Acta* 2006; **52**: 1563–6.
50. Peng HJ, Xu WT and Zhu L *et al.* 3D carbonaceous current collectors: the origin of enhanced cycling stability for high-sulfur-loading lithium–sulfur batteries. *Adv Funct Mater* 2016; **26**: 6351–8.
51. Jin S, Xin S and Wang L *et al.* Covalently-connected carbon nanostructures for 3D current collectors in both cathode and anode of Li–S batteries. *Adv Mater* 2016; **28**: 9094–102.
52. Zhang B, Qin X and Li GR *et al.* Enhancement of long stability of sulfur cathode by encapsulating sulfur into micropores of carbon spheres. *Energy Environ Sci* 2010; **3**: 1531–7.
53. Li Z, Yuan L and Yi Z *et al.* Insight into the electrode mechanism in lithium–sulfur batteries with ordered microporous carbon confined sulfur as the cathode. *Adv Energy Mater* 2014; **4**: 1301473.
54. Xin S, Yu L and You Y *et al.* The electrochemistry with lithium versus sodium of selenium confined to slit micropores in carbon. *Nano Lett* 2016; **16**: 4560–8.
55. Whittingham MS. Lithium batteries and cathode materials. *Chem Rev* 2004; **104**: 4271–302.
56. Yang Y, McDowell MT and Jackson A *et al.* New nanostructured Li<sub>2</sub>S/silicon rechargeable battery with high specific energy. *Nano Lett* 2010; **10**: 1486–91.
57. Yang Y, Zheng G and Misra S *et al.* High-capacity micrometer-sized Li<sub>2</sub>S particles as cathode materials for advanced rechargeable lithium–ion batteries. *J Am Chem Soc* 2012; **134**: 15387–94.
58. Fu Y, Su YS and Manthiram A. Highly reversible lithium/dissolved polysulfide batteries with carbon nanotube electrodes. *Angew Chem Int Ed* 2013; **52**: 6930–5.
59. Su YS, Fu Y and Guo B *et al.* Fast, reversible lithium storage with a sulfur/long-chain–polysulfide redox couple. *Chem – Eur J* 2013; **19**: 8621–6.
60. Fanous J, Wegner M and Grimminger J *et al.* Structure-related electrochemistry of sulfur–poly(acrylonitrile) composite cathode materials for rechargeable lithium batteries. *Chem Mater* 2011; **23**: 5024–8.
61. Wang J, Yang J and Xie J *et al.* A novel conductive polymer–sulfur composite cathode material for rechargeable lithium batteries. *Adv Mater* 2002; **14**: 963–5.

62. Wang JL, Yang J and Xie JY *et al.* Sulfur-carbon nano-composite as cathode for rechargeable lithium battery based on gel electrolyte. *Electrochem Commun* 2002; **4**: 499–502.
63. Xu Z, Wang J and Yang J *et al.* Enhanced performance of a lithium-sulfur battery using a carbonate-based electrolyte. *Angew Chem Int Ed* 2016; **55**: 10372–5.
64. Yan K, Lee HW and Gao T *et al.* Ultrathin two-dimensional atomic crystals as stable interfacial layer for improvement of lithium metal anode. *Nano Lett* 2014; **14**: 6016–22.
65. Zheng G, Lee SW and Liang Z *et al.* Interconnected hollow carbon nanospheres for stable lithium metal anodes. *Nat Nanotech* 2014; **9**: 618–23.
66. Huang C, Xiao J and Shao Y *et al.* Manipulating surface reactions in lithium-sulphur batteries using hybrid anode structures. *Nat Commun* 2014; **5**: 3015.
67. Ding F, Xu W and Graff GL *et al.* Dendrite-free lithium deposition via self-healing electrostatic shield mechanism. *J Am Chem Soc* 2013; **135**: 4450–6.
68. Yang CP, Yin YX and Zhang SF *et al.* Accommodating lithium into 3D current collectors with a submicron skeleton towards long-life lithium metal anodes. *Nat Commun* 2015; **6**: 8058.
69. Zhou W, Wang S and Li Y *et al.* Plating a dendrite-free lithium anode with a polymer/ceramic/polymer sandwich electrolyte. *J Am Chem Soc* 2016; **138**: 9385–8.
70. Li W, Yao H and Yan K *et al.* The synergetic effect of lithium polysulfide and lithium nitrate to prevent lithium dendrite growth. *Nat Commun* 2015; **6**: 7436.
71. Goodenough JB and Park KS. The Li-ion rechargeable battery: a perspective. *J Am Chem Soc* 2013; **135**: 1167–76.
72. Xiong S, Xie K and Diaoy Y *et al.* Characterization of the solid electrolyte interphase on lithium anode for preventing the shuttle mechanism in lithium-sulfur batteries. *J Power Sources* 2014; **246**: 840–5.
73. Zhang SS. Effect of discharge cutoff voltage on reversibility of lithium/sulfur batteries with LiNO<sub>3</sub>-contained electrolyte. *J Electrochem Soc* 2012; **159**: A920–3.
74. Zhang SS. Role of LiNO<sub>3</sub> in rechargeable lithium/sulfur battery. *Electrochim Acta* 2012; **70**: 344–8.
75. Li NW, Yin YX and Yang CP *et al.* An artificial solid electrolyte interphase layer for stable lithium metal anodes. *Adv Mater* 2016; **28**: 1853–8.
76. Xin S, Yin YX and Guo YG *et al.* A high-energy room-temperature sodium-sulfur battery. *Adv Mater* 2014; **26**: 1261–5.
77. Xu J, Xin S and Liu JW *et al.* Elastic carbon nanotube aerogel meets tellurium nanowires: a binder- and collector-free electrode for Li-Te batteries. *Adv Funct Mater* 2016; **26**: 3580–8.
78. Yang CP, Xin S and Yin YX *et al.* An advanced selenium-carbon cathode for rechargeable lithium-selenium batteries. *Angew Chem Int Ed* 2013; **52**: 8363–7.
79. Zhang J, Yin YX and Guo YG. High-capacity Te anode confined in microporous carbon for long-life Na-ion batteries. *ACS Appl Mater Interfaces* 2015; **7**: 27838–44.
80. Zhang J, Yin YX and You Y *et al.* A high-capacity Tellurium@Carbon anode material for lithium-ion batteries. *Energy Technol* 2014; **2**: 757–62.
81. Ye H, Yin YX and Zhang SF *et al.* Advanced Se-C nanocomposites: a bifunctional electrode material for both Li-Se and Li-ion batteries. *J Mater Chem A* 2014; **2**: 13293–8.
82. Xu J, Xu J and Wang Z *et al.* Synthesis of perovskite-based porous La<sub>0.75</sub>Sr<sub>0.25</sub>MnO<sub>3</sub> nanotubes as a highly efficient electrocatalyst for rechargeable lithium-oxygen batteries. *Angew Chem Int Ed* 2013; **14**: 3887–90.
83. Peng Z, Freunberger S and Chen Y *et al.* A reversible and higher-rate Li-O<sub>2</sub> battery. *Science* 2012; **6094**: 563–6.
84. Shui J, Okasinski J and Kensesei P *et al.* Reversibility of anodic lithium in rechargeable lithium-oxygen batteries. *Nat Commun* 2013; **4**: 2255.
85. Chen Y, Freunberger S and Peng Z *et al.* Li-O<sub>2</sub> battery with a dimethylformamide electrolyte. *J Am Chem Soc* 2012; **18**: 7952–7.
86. Aurbach D, McCloskey BD and Nazar LF *et al.* Advances in understanding mechanisms underpinning lithium-air batteries. *Nat Energy* 2016; **1**: 16128.
87. Li Y, Wang X and Dong S *et al.* Recent advances in non-aqueous electrolyte for rechargeable Li-O<sub>2</sub> batteries. *Adv Energy Mater* 2016; **6**: 1600751.
88. Yao X, Dong Q and Cheng Q *et al.* Why do lithium-oxygen batteries fail: parasitic chemical reactions and their synergistic effect. *Angew Chem Int Ed* 2016; **55**: 2–12.
89. Xu J, Wang Z and Xu D *et al.* Tailoring deposition and morphology of discharge products towards high-rate and long-life lithium-oxygen batteries. *Nat Commun* 2013; **4**: 2438.
90. Luntz AC and McCloskey BD. Nonaqueous Li-air batteries: a status report. *Chem Rev* 2014; **114**: 11721–50.
91. Lu J, Li L and Park J B *et al.* Aprotic and aqueous Li-O<sub>2</sub> batteries. *Chem Rev* 2014; **114**: 5611–40.
92. Liu T, Leslkes M and Yu W *et al.* Cycling Li-O<sub>2</sub> batteries via LiOH formation and decomposition. *Science* 2015; **350**: 530–3.
93. Lu YC and Yang SH. Probing the reaction kinetics of the charge reactions of nonaqueous Li-O<sub>2</sub> batteries. *J Phys Chem Lett* 2013; **4**: 93–9.
94. Guo Z, Zhou D and Dong X *et al.* Ordered hierarchical mesoporous/macroporous carbon: a high-performance catalyst for rechargeable Li-O<sub>2</sub> batteries. *Adv Mater* 2013; **25**: 5668–72.
95. Zhao C, Yu C and Liu S *et al.* 3D porous N-doped graphene frameworks made of interconnected nanocages for ultrahigh-rate and long-life Li-O<sub>2</sub> batteries. *Adv Funct Mater* 2015; **44**: 6913–20.
96. Han J, Guo X and Ito Y *et al.* Effect of chemical doping on cathodic performance of bicontinuous nanoporous graphene for Li-O<sub>2</sub> batteries. *Adv Energy Mater* 2016; **6**: 1501870.
97. Wang ZL, Xu JJ and Zhang LL *et al.* Graphene oxide gel-derived, free-standing, hierarchically porous carbon for high-capacity and high-rate rechargeable Li-O<sub>2</sub> batteries. *Adv Funct Mater* 2012; **17**: 3699–705.
98. Lim HD, Park KY and Song H *et al.* Enhanced power and rechargeability of a Li-O<sub>2</sub> battery based on a hierarchical-fibril CNT electrode. *Adv Mater* 2013; **9**: 1348–52.
99. Ganapathy S, Adams BD and Stenou G *et al.* Nature of Li<sub>2</sub>O<sub>2</sub> oxidation in a Li-O<sub>2</sub> battery revealed by operando X-ray diffraction. *J Am Chem Soc* 2014; **46**: 16335–44.
100. Ma S, Wu Y and Wang J *et al.* Reversibility of noble metal-catalyzed aprotic Li-O<sub>2</sub> batteries. *Nano Lett* 2015; **12**: 8084–90.
101. Yang C, Wong R and Hong M *et al.* Unexpected Li<sub>2</sub>O<sub>2</sub> film growth on carbon nanotube electrodes with CeO<sub>2</sub> nanoparticles in Li-O<sub>2</sub> batteries. *Nano Lett* 2016; **16**: 2969–74.
102. Zhang K, Zhang L and Chen X *et al.* Mesoporous cobalt molybdenum nitride: a highly active bifunctional electrocatalyst and its application in lithium-O<sub>2</sub> batteries. *J Phys Chem C* 2013; **2**: 858–65.
103. Suntivich J, Gasteiger HA and Yanbuuchi N *et al.* Design principles for oxygen-reduction activity on perovskite oxide catalysts for fuel cells and metal-air batteries. *Nat Chem* 2011; **3**: 546–50.
104. Oh SH, Black R and Pomerantseva E *et al.* Synthesis of a metallic mesoporous pyrochlore as a catalyst for lithium-O<sub>2</sub> batteries. *Nat Chem* 2012; **4**: 1004–10.
105. Zhong L, Mitchell RR and Liu Y *et al.* In situ transmission electron microscopy observations of electrochemical oxidation of Li<sub>2</sub>O<sub>2</sub>. *Nano Lett* 2013; **5**: 2209–14.

106. Gallant BM, Kwabi DG and Mitchell RR *et al.* Influence of  $\text{Li}_2\text{O}_2$  morphology on oxygen reduction and evolution kinetics in  $\text{Li}-\text{O}_2$  batteries. *Energy Environ Sci* 2013; **6**: 2518–28.
107. Lu YC, Gasteiger HA and Crumlin E *et al.* Electrocatalytic activity studies of select metal surfaces and implications in  $\text{Li}-\text{air}$  batteries. *J Electrochem Soc* 2010; **9**: A1016–25.
108. Huang X, Yu H and Tan H *et al.* Carbon nanotube-encapsulated noble metal nanoparticle hybrid as a cathode material for  $\text{Li}-\text{oxygen}$  batteries. *Adv Funct Mater* 2014; **41**: 6516–23.
109. Tian F, Radin MD and Siegel DJ. Enhanced charge transport in amorphous  $\text{Li}_2\text{O}_2$ . *Chem Mater* 2014; **26**: 2952–9.
110. Radin MD, Rodriguez JF and Tian F *et al.* Lithium peroxide surfaces are metallic, while lithium oxide surfaces Are Not. *J Am Chem Soc* 2012; **134**: 1093–103.
111. Yilmaz E, Yogi C and Yamanaka K *et al.* Promoting formation of noncrystalline  $\text{Li}_2\text{O}_2$  in the  $\text{Li}-\text{O}_2$  battery with  $\text{RuO}_2$  nanoparticles. *Nano Lett* 2013; **13**: 4679–84.
112. Chen Y, Freunberger SA and Peng Z *et al.* Charging a  $\text{Li}-\text{O}_2$  battery using a redox mediator. *Nat Chem* 2012; **4**: 1004–10.
113. Lim HD, Song H and Kim J *et al.* Superior rechargeability and efficiency of lithium–oxygen batteries: hierarchical air electrode architecture combined with a soluble catalyst. *Angew Chem Int Ed* 2014; **53**: 3926–31.
114. Bergner BJ, Schürmann A and Pepler K *et al.* TEMPO: a mobile catalyst for rechargeable  $\text{Li}-\text{O}_2$  batteries. *J Am Chem Soc* 2014; **136**: 15054–64.
115. Sun D, Shen Y and Zhang W *et al.* A solution-phase bifunctional catalyst for lithium–oxygen batteries. *J Am Chem Soc* 2014; **136**: 8941–6.
116. Lim HD, Lee B and Zheng Y *et al.* Rational design of redox mediators for advanced  $\text{Li}-\text{O}_2$  batteries *Nat Energy* 2016; **1**: 16066.
117. Xu W, Wang J and Ding F *et al.* Lithium metal anodes for rechargeable batteries. *Energy Environ Sci* 2014; **7**: 513–37.
118. Shui JD, Okasinski JS and Kenesei P *et al.* Reversibility of anodic lithium in rechargeable lithium–oxygen batteries. *Nat Commun* 2013; **4**: 2255.
119. Walker W, Giordani V and Uddin J *et al.* A rechargeable  $\text{Li}-\text{O}_2$  battery using a lithium nitrate/N,N–dimethylacetamide electrolyte. *J Am Chem Soc* 2013; **135**: 2076–9.
120. Shui JD, Okasinski JS and Kenesei P *et al.* Composite protective layer for Li metal anode in high-performance lithium–oxygen batteries. *Electrochem Commun* 2014; **40**: 45–8.
121. Kang SJ, Mori T and Suk J *et al.* Improved cycle efficiency of lithium metal electrodes in  $\text{Li}-\text{O}_2$  batteries by a two-dimensionally ordered nanoporous separator. *J Mater Chem A* 2014; **2**: 9970–4.
122. Peng Z, Freunberger SA and Chen Y *et al.* A reversible and higher-rate  $\text{Li}-\text{O}_2$  battery. *Science* 2012; **337**: 563–6.
123. Hassoun J, Jung HG and Lee DJ *et al.* A metal-free, lithium–ion oxygen battery: a step forward to safety in lithium–air batteries. *Nano Lett* 2012; **11**: 5775–9.
124. Liu QC, Xu JJ and Yuan S *et al.* Artificial protection film on lithium metal anode toward long-cycle-life lithium–oxygen batteries. *Adv Mater* 2015; **27**: 5241–7.
125. Gallant BM, Mitchell RR and Kwabi DG *et al.* Chemical and morphological changes of  $\text{Li}-\text{O}_2$  battery electrodes upon cycling. *J Phys Chem C* 2012; **39**: 20800–5.
126. Jian Z, Liu P and Li F *et al.* Core–shell-structured  $\text{CNT@RuO}_2$  composite as a high-performance cathode catalyst for rechargeable  $\text{Li}-\text{O}_2$  batteries. *Angew Chem Int Ed* 2014; **2**: 442–6.
127. Xie J, Yao X and Cheng Q *et al.* Three dimensionally ordered mesoporous carbon as a stable, high-performance  $\text{Li}-\text{O}_2$  battery cathode. *Angew Chem Int Ed* 2014; **127**: 4373–7.
128. Zhou W, Zhang H and Nie H *et al.* Hierarchical micron-sized mesoporous/macroporous graphene with well-tuned surface oxygen chemistry for high capacity and cycling stability  $\text{Li}-\text{O}_2$  battery. *ACS Appl Mater Interfaces* 2015; **5**: 3389–97.
129. Li F, Tang DM and Chen Y *et al.* Ru/ITO: A carbon-free cathode for nonaqueous  $\text{Li}-\text{O}_2$  battery. *Nano Lett* 2013; **13**: 4702–7.
130. Zhao G, Mo R and Wang B *et al.* Enhanced cyclability of  $\text{Li}-\text{O}_2$  batteries based on  $\text{TiO}_2$  supported cathodes with no carbon or binder. *Chem Mater* 2014; **26**: 2551–6.
131. Li F, Tang DM and Zhang T *et al.* Superior performance of a  $\text{Li}-\text{O}_2$  battery with metallic  $\text{RuO}_2$  hollow spheres as the carbon-free cathode. *Adv Energy Mater* 2015; **5**: 1500294.
132. Xie J, Yao X and Madden IP *et al.* Selective deposition of Ru nanoparticles on  $\text{TiSi}_2$  nanonet and its utilization for  $\text{Li}_2\text{O}_2$  formation and decomposition. *J Am Chem Soc* 2014; **136**: 8903–6.
133. Thotiyil MMO, Freunberger SA and Peng Z *et al.* A stable cathode for the aprotic  $\text{Li}-\text{O}_2$  battery. *Nat Mater* 2013; **12**: 1050–6.
134. Kundu D, Black R and Berg EJ *et al.* A highly active nanostructured metallic oxide cathode for aprotic  $\text{Li}-\text{O}_2$  batteries. *Energy Environ Sci* 2015; **8**: 1292–8.
135. Jung HG, Hassoun J and Park JB *et al.* An improved high-performance lithium–air battery. *J Am Chem Soc* 2012; **18**: 7952–7.
136. McCloskey BD, Bethune DS and Shelby RM *et al.* Solvents' critical role in nonaqueous lithium–oxygen battery electrochemistry. *J Phys Chem Lett* 2011; **2**: 1161–6.
137. Freunberger SA, Chen Y and Drewett NE *et al.* The lithium–oxygen battery with ether-based electrolytes. *Angew Chem Int Ed* 2011; **37**: 8609–13.
138. Hartmann P, Bender CL and Vračar M *et al.* A rechargeable room-temperature sodium superoxide ( $\text{NaO}_2$ ) battery. *Nat Mater* 2013; **12**: 228–32.
139. Xue L, Gao H and Zhou W *et al.* Liquid K–Na alloy anode enables dendrite-free potassium battery. *Adv Mater* 2016; **28**: 9608–12.
140. Zhao-Karger Z, Zhao X and Wang D *et al.* Performance improvement of magnesium sulfur batteries with modified non-nucleophilic electrolytes. *Adv Energy Mater* 2015; **5**: 1401155.
141. Gao T, Li X and Wang X *et al.* A rechargeable Al/s battery with an ionic-liquid electrolyte. *Angew Chem Int Ed* 2016; **55**: 9898–901.
142. Fu G, Chen Y and Cui Z *et al.* Novel hydrogel-derived bifunctional oxygen electrocatalyst for rechargeable air cathodes. *Nano Lett* 2016; **16**: 6516–22.